

# Supramolecular crystal of Mn(15-Crown-5)(MnCl<sub>4</sub>)(DMF) with dielectric phase transition, high quantum yield and phase transition-induced luminescence enhancement behavior

Guo-Jun Yuan<sup>\*ab</sup> Xue-Wei Pan<sup>a</sup> Li Chen<sup>d</sup> Chao Chen<sup>d</sup> Xiao-Ming Ren<sup>\*a,c</sup>

<sup>a</sup> State Key Laboratory of Materials-Oriented Chemical Engineering and College of Chemistry and molecular of Engineering, Nanjing Tech University, Nanjing 211816, P. R. China

<sup>b</sup> Department of Chemistry, Nanjing Xiaozhuang University, Nanjing 211171, P. R. China

<sup>c</sup> State Key Laboratory of Coordination Chemistry, Nanjing University, Nanjing 210023, P. R. China

<sup>d</sup> Goldenway Environmental Technology Co., Ltd, Nanjing 211121, P. R. China

Tel.: +86 25 58139476

Email: [ahchljygj@163.com](mailto:ahchljygj@163.com) (GJY); [xmren@njtech.edu.cn](mailto:xmren@njtech.edu.cn) (XMR)

## Contents

Table S1: Crystal data and structure refinements for **1** at 150, 298 and 360 K

Table S2: The shorter Cl...H contacts in the charge-assisted H-bonds of **1** at 150 K, 298 K and 360 K

Table S3: The parameters of  $U_{eq}$  in **1** at 150, 298 and 360 K

Table S4: CIE chromaticity of **1** at different temperatures

Figure S1: Comparison of simulated and experimental Powder X-ray diffraction profiles for **1**.

Figure S2: (a) A molecular monolayer of Mn(15-Crown-5)(MnCl<sub>4</sub>)(DMF) for **1** at 150 K; (b–d) Packing diagram viewed along the a-axes, b-axes and c-axes, respectively, for **1** at 150 K.

Figure S3: (a) A molecular monolayer of Mn(15-Crown-5)(MnCl<sub>4</sub>)(DMF) for **1** at 298 K; (b–d) Packing diagram viewed along the a-axes, b-axes and c-axes, respectively, for **1** at 298 K.

Figure S4: (a) A molecular monolayer of Mn(15-Crown-5)(MnCl<sub>4</sub>)(DMF) for **1** at 360 K; (b–d) Packing diagram viewed along the a-axes, b-axes and c-axes, respectively, for **1** at 360 K.

Figure S5: (a–b) Plots of  $\epsilon'$  vs. temperature in the 150–365 K range; (c–e) Plots of the electric modulus imaginary part versus frequency for **1**; (f) Arrhenius plot for dielectric relaxation in the 203–253 K range for **1**.

Figure S6: ORTEP plots of **1** at 150, 298 and 360 K where the atom displacement ellipsoids are drawn at 50% probability level, indicating that the anisotropic displacements of the Cl1–Cl4 in MnCl<sub>4</sub><sup>2-</sup> coordinated tetrahedron, as well as the O6 and two terminal methyl' C atoms in DMF increase with temperature elevated.

Figure S7: The image for **1** at 303 K with natural light.

Figure S8: (a–f) The variable-temperature images for **1** in the sequence of 303, 320, 340, 350, 360 and 380 K with excitation at 365 nm.

Table S5: Comparison of Mn–Cl bond length (Å), quantum yield (QY, %) and lifetime ( $\tau$ ,  $\mu$ S) in the compounds containing MnCl<sub>4</sub><sup>2-</sup> tetrahedron in literature and this work

Table S1: Crystal data and structure refinements for **1** at 150, 298 and 360 K

Temp./K	150 K	298 K	360 K
Formula	C <sub>13</sub> H <sub>27</sub> O <sub>6</sub> NMn <sub>2</sub> Cl <sub>4</sub>	C <sub>13</sub> H <sub>27</sub> O <sub>6</sub> NMn <sub>2</sub> Cl <sub>4</sub>	C <sub>13</sub> H <sub>27</sub> O <sub>6</sub> NMn <sub>2</sub> Cl <sub>4</sub>
SG	<i>P</i> 2 <sub>1</sub> 2 <sub>1</sub> 2 <sub>1</sub>	<i>P</i> 2 <sub>1</sub> 2 <sub>1</sub> 2 <sub>1</sub>	<i>P</i> 2 <sub>1</sub> 2 <sub>1</sub> 2 <sub>1</sub>
CCDC no.	2281549	2281551	2281552
Crystal system	Orthorhombic	Orthorhombic	Orthorhombic
a (Å)	10.4466(4)	10.2522(4)	10.292(2)
b (Å)	14.3125(6)	14.7124(7)	14.750 (4)
c (Å)	14.7885(7)	15.6349(8)	15.679(4)
α (°)	90	90	90
β (°)	90	90	90
γ (°)	90	90	90
V(Å <sup>3</sup> )/Z	2211.13(16)/4	2358.28(19)/4	2380.2(10)/4
ρ (g·cm <sup>-3</sup> )	1.637	1.535	1.521
F(000)	1112	1112	1112
Abs. coeff. (mm <sup>-1</sup> )	1.652	1.549	1.535
θ Ranges/°	2.39-26.33	2.42-22.35	2.37-22.27
Index ranges	-12 ≤ h ≤ 11	-11 ≤ h ≤ 11	-11 ≤ h ≤ 12
	-16 ≤ k ≤ 17	-16 ≤ k ≤ 17	-16 ≤ k ≤ 17
	-16 ≤ l ≤ 17	-18 ≤ l ≤ 18	-18 ≤ l ≤ 18
R <sub>int</sub>	0.0322	0.0484	0.0549
Indep. refl/ restr. /para.	3887/24/256	4131/764/373	4186/798/373
Goodness of fit on F <sup>2</sup>	1.065	1.065	1.047
R <sub>1</sub> , wR <sub>2</sub> [I > 2σ(I)]	0.0276 0.0508	0.0517 0.1064	0.0620 0.1475
R <sub>1</sub> , wR <sub>2</sub> [all data]	0.0355 0.0545	0.0876 0.1295	0.1072 0.1832
Residual (e·Å <sup>-3</sup> )	0.335/ -0.258	0.564/ -0.391	0.429/ -0.382

$$R_1 = \frac{\sum ||F_o| - |F_c||}{\sum |F_o|}, wR_2 = \left[ \frac{\sum w(\sum F_o^2 - F_c^2)^2}{\sum w(F_o^2)^2} \right]^{1/2}$$

Table S2: The shorter Cl...H contacts in the charge-assisted H-bonds of **1** at 150 K, 298 K and 360 K

150 K		298 K		360 K	
Atom pair	Distance / Å	Atom pair	Distance / Å	Atom pair	Distance / Å
Cl2...H12C	2.876	Cl2...H2AB	2.906	Cl2...H13B	2.825
Cl2...H13C	2.938	Cl2...H8B	2.926	Cl4...H4AB	2.807
Cl4...H10A	2.948	Cl2...H12C	2.776	Cl4...H7AB	2.640
Cl4...H12A	2.905	Cl4...H2A	2.695		
		Cl4...H2AA	2.892		

Table S3: The parameters of  $U_{eq}$  in **1** at 150, 298 and 360 K

Non-H atom	$U_{eq}(150K)$	$U_{eq}(298K)$	$U_{eq}(360K)$
Mn1	0.02387(14)	0.0521(4)	0.0628(5)
Mn2	0.03137(16)	0.0597(4)	0.0686(6)
Cl1	0.0340(2)	0.0649(7)	0.0759(9)
Cl2	0.0464(3)	0.0911(10)	0.1056(13)
Cl3	0.0428(3)	0.0887(9)	0.152(2)
Cl4	0.0544(3)	0.1361(16)	0.1051(13)
N1	0.0307(8)	0.096(3)	0.134(4)
O1	0.0306(7)	0.081(3)	0.113(4)
O1A		0.110(9)	0.105(9)
O2	0.0305(7)	0.075(3)	0.104(4)
O2A		0.094(9)	0.123(9)
O3	0.0365(7)	0.085(3)	0.091(4)
O3A		0.090(8)	0.119(9)
O4	0.0354(7)	0.079(3)	0.100(4)
O4A		0.089(8)	0.105(9)
O5	0.0362(7)	0.096(4)	0.099(4)
O5A		0.100(8)	0.103(9)
O6	0.0337(7)	0.093(3)	0.106(3)
C1	0.0349(11)	0.089(4)	0.123(6)
C1A		0.110(9)	0.124(10)
C2	0.0346(10)	0.082(4)	0.131(6)
C2A		0.091(9)	0.123(10)
C3	0.0384(11)	0.082(4)	0.114(6)
C3A		0.096(9)	0.128(10)
C4	0.0411(12)	0.092(4)	0.107(5)
C4A		0.091(9)	0.119(10)
C5	0.0437(12)	0.088(4)	0.117(6)
C5A		0.094(9)	0.117(10)
C6	0.0468(13)	0.088(4)	0.114(6)
C6A		0.098(9)	0.110(10)
C7	0.043(3)	0.092(5)	0.119(6)
C7A	0.037(4)	0.093(9)	0.112(9)
C8	0.042(4)	0.108(5)	0.109(5)
C8A	0.039(4)	0.095(9)	0.111(10)
C9	0.0417(12)	0.107(6)	0.115(6)
C9A		0.113(9)	0.103(9)
C10	0.0376(11)	0.114(5)	0.132(6)
C10A		0.109(9)	0.109(10)
C11	0.0325(10)	0.107(4)	0.122(5)
C12	0.0450(13)	0.145(7)	0.164(8)
C13	0.0508(14)	0.163(7)	0.152(7)

Table S4: CIE chromaticity of **1** at different temperatures

Temperature	CIE x	CIE y	X	Y	Z
180 K	0.48504	0.35971	35466.2689	18909.6024	16236.621
200 K	0.48062	0.34637	34772.6817	20154.6555	13721.4035
250 K	0.46272	0.33254	34308.4075	20042.8811	10242.0789
280 K	0.46571	0.32714	34813.1758	21639.2838	9926.50191
310 K	0.56386	0.43064	36235.7751	17606.2353	48302.6245
340 K	0.52759	0.39617	38743.5563	19877.6443	29325.5228
360 K	0.57173	0.42203	45553.2397	24628.1124	59826.5936
380 K	0.57171	0.41955	45841.8025	25217.6891	57917.3342

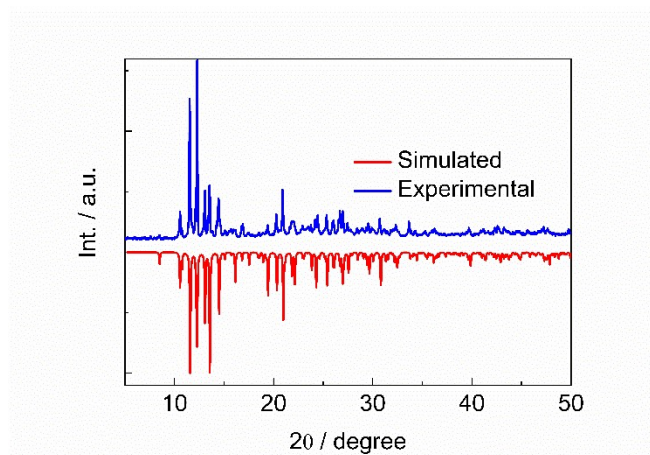


Figure S1: Comparison of simulated and experimental Powder X-ray diffraction profiles for **1**.

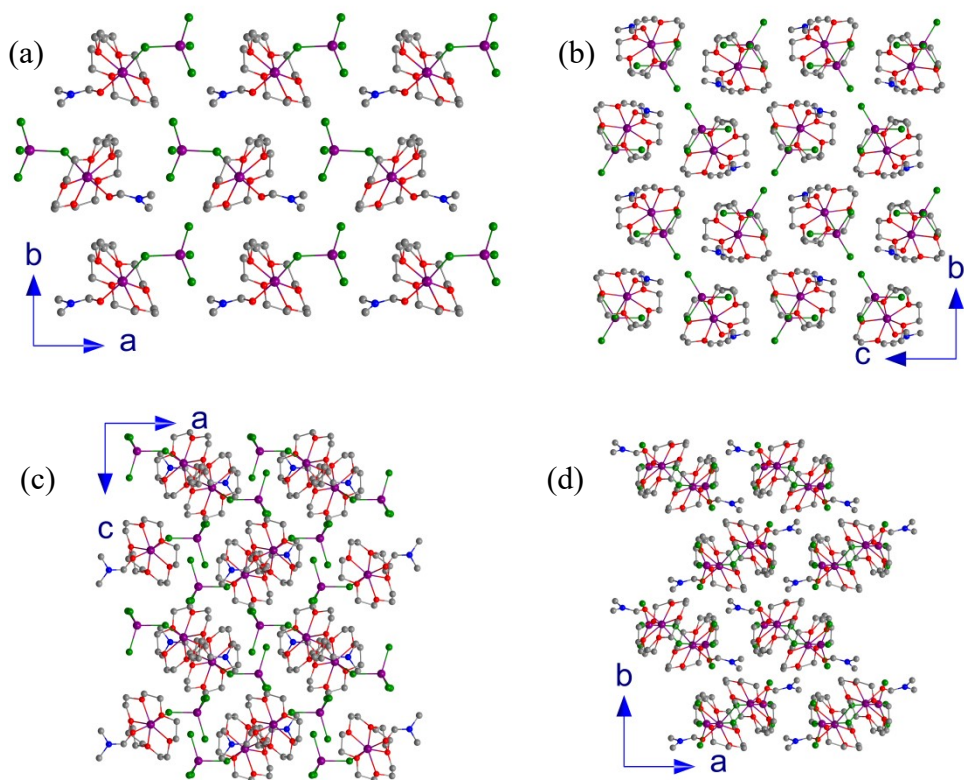


Figure S2: (a) A molecular monolayer of Mn(15-Crown-5)(MnCl<sub>4</sub>)(DMF) for **1** at 150 K; (b–d) Packing diagram viewed along the a-axes, b-axes and c-axes, respectively, for **1** at 150 K.

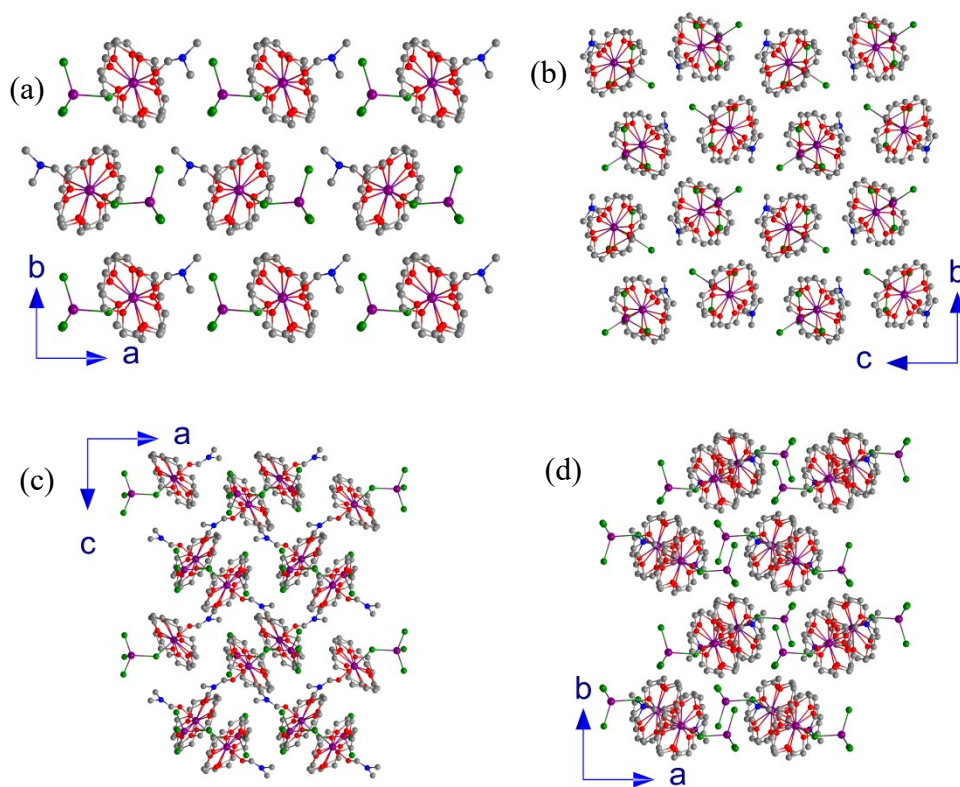


Figure S3: (a) A molecular monolayer of Mn(15-Crown-5)(MnCl<sub>4</sub>)(DMF) for **1** at 298 K; (b–d) Packing diagram viewed along the a-axes, b-axes and c-axes, respectively, for **1** at 298 K.



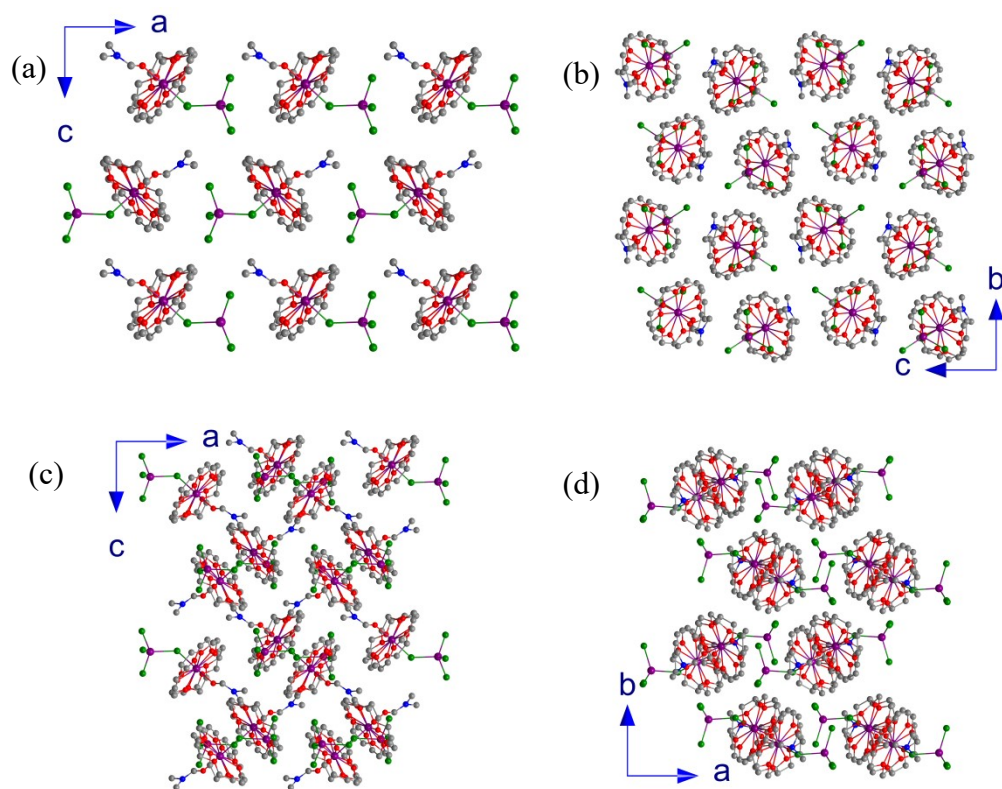


Figure S4: (a) A molecular monolayer of Mn(15-Crown-5)(MnCl<sub>4</sub>)(DMF) for **1** at 360 K; (b–d) Packing diagram viewed along the a-axes, b-axes and c-axes, respectively, for **1** at 360 K.

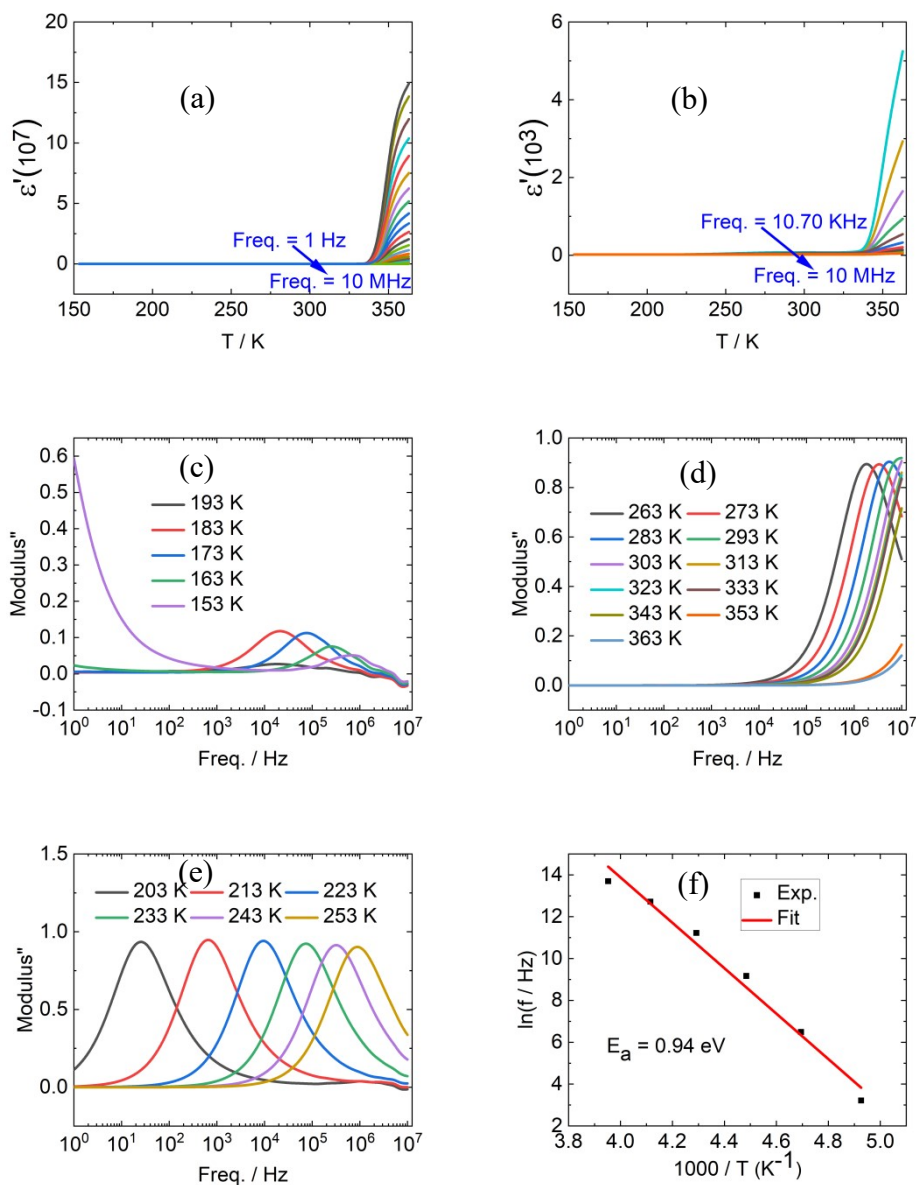


Figure S5: (a–b) Plots of  $\epsilon'$  vs. temperature in the 150–365 K range; (c–e) Plots of the electric modulus imaginary part versus frequency for **1**; (f) Arrhenius plot for dielectric relaxation in the 203–253 K range for **1**.

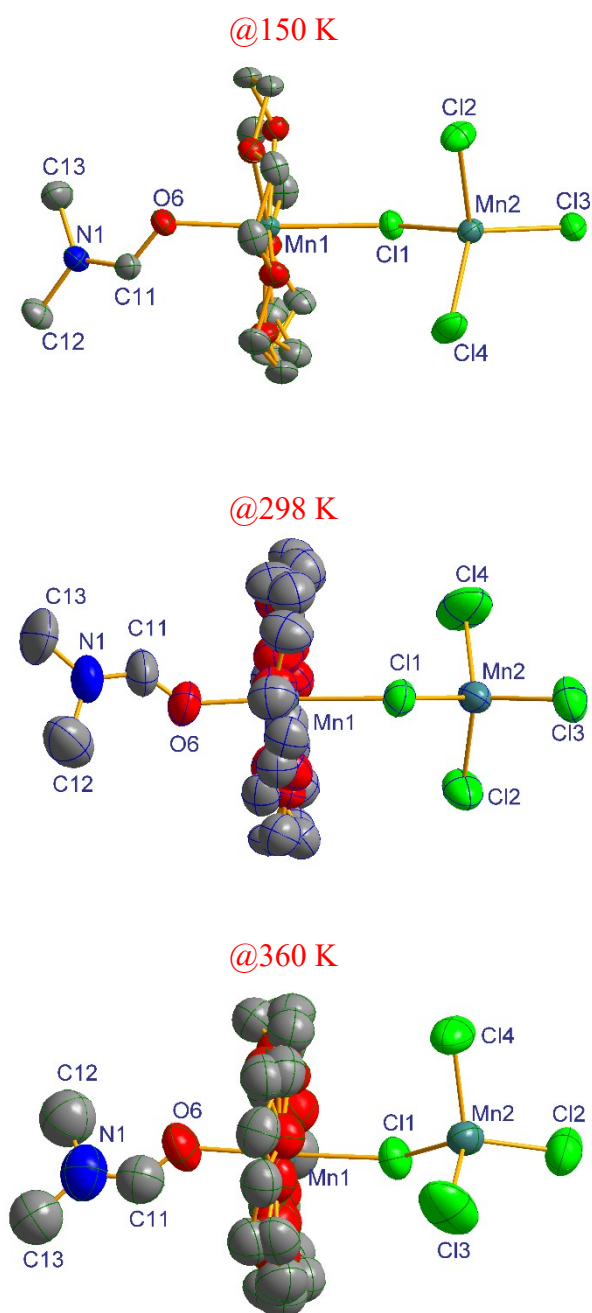


Figure S6: ORTEP plots of **1** at 150, 298 and 360 K where the atom displacement ellipsoids are drawn at 50% probability level, indicating that the anisotropic displacements of the C11–C14 in  $\text{MnCl}_4^{2-}$  coordinated tetrahedron, as well as the O6 and two terminal methyl' C atoms in DMF increase with temperature elevated.

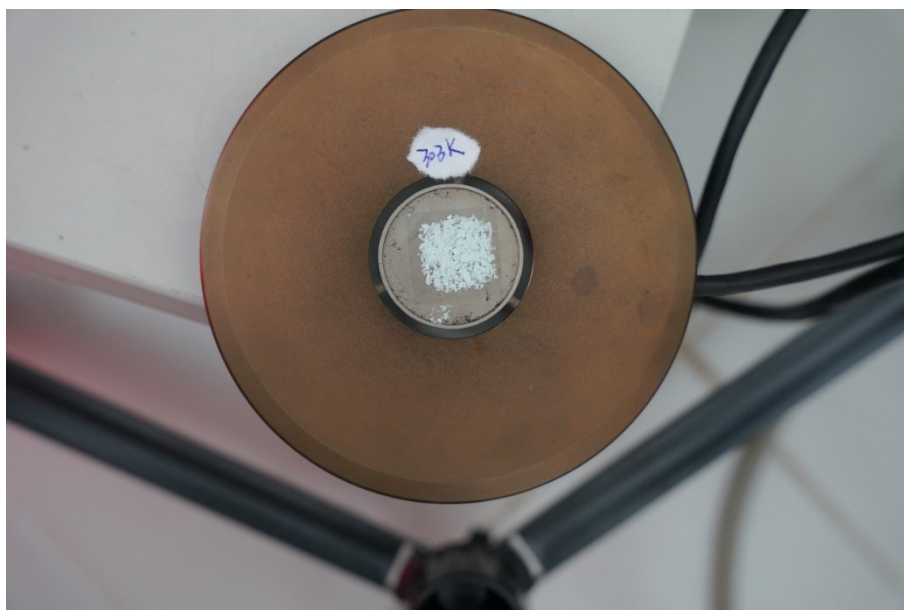


Figure S7: The image for **1** at 303 K with natural light.

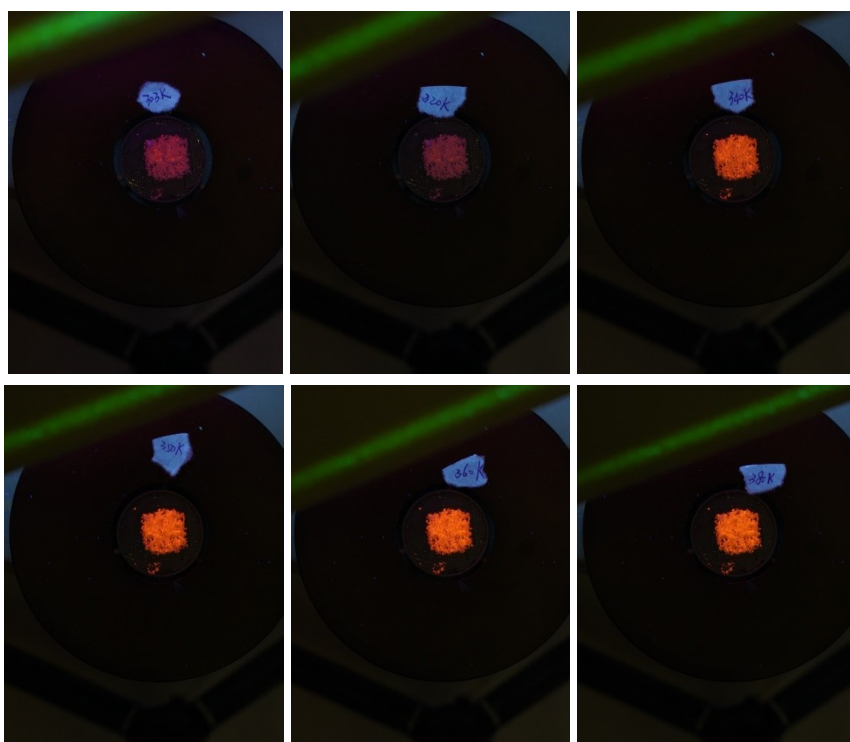


Figure S8: (a-f) The variable-temperature images for **1** in the sequence of 303, 320, 340, 350, 360 and 380 K with excitation at 365 nm.

Table S5: Comparison of Mn–Cl bond length (Å), quantum yield (QY, %) and lifetime ( $\tau$ ,  $\mu$ S) in the compounds containing  $\text{MnCl}_4^{2-}$  tetrahedron in literature and this work

Compound	QY (%) / $\tau$ ( $\mu$ S)	Mn-Cl Bond Length (Å)	Ref.
$[(\text{TEA})(\text{TMA})]\text{MnCl}_4$	99/3.74	2.3699(11) 2.3696(7) 2.3696(7) 2.3632(9)	Inorg. Chem., 2023, 62, 5791–5798.
$[(\text{TPA})(\text{TMA})_3](\text{MnCl}_4)_2$	66/3.63	2.3728(14) 2.3649(15) 2.3572(17) 2.3568(17)	Inorg. Chem., 2023, 62, 5791–5798.
$(\text{Piperidinium})_3\text{Cl}[\text{MnCl}_4]$	54.5/3500.0	2.3861(5) 2.3694(5) 2.3687(5) 2.3312(5)	Inorg. Chem., 2023, 62, 3202–3211.
$(3\text{-CNDA})_2\text{MnCl}_4$	20.55/600	2.3973(6) 2.3628(6) 2.3390(6) 2.3338(6)	Dalton Trans., 2022, 51, 14408–14412.
$[\text{TMAA}]_2[\text{MnCl}_4]$	35.19/–	2.3701(10) 2.3679(10) 2.3639(10) 2.3551(11)	Dalton. Trans., 2022, 51, 2005–2011
$[\text{Me}_3\text{NCH}_2\text{CH}_2\text{F}]_2\text{MnCl}_4$	41.1/–	2.3761(14) 2.3738(13) 2.3695(13) 2.3591(13)	New J. Chem., 2022, 46, 20005–20009.
$(\text{C}_5\text{H}_8\text{N}_2)_2\text{MnCl}_4$	79.77/–	2.371(3) 2.369(3) 2.351(3) 2.348(3)	CrystEngComm, 2022,24,6910–6916.
$[\text{DMAEMP}]\text{MnCl}_4$	81.11/3260.0	2.3859(8) 2.3712(8) 2.3503(8) 2.3369(7)	Chem. Commun., 2021,57,6907–6910.
$[\text{PDMI}]\text{MnCl}_4$	42.49/3527.0	2.395(17) 2.373(6) 2.35(3) 2.35(3)	Chem. Commun., 2021,57,6907–6910.
$[\text{MP}]_2\text{MnCl}_4 \cdot 2\text{Cl}$	19.96/2890	2.3913(7)	Chem. Commun., 2021,57,6907–6910.

		2.3620(7)	
		2.3550(6)	
		2.3516(7)	
[DMP]MnCl <sub>4</sub>	13.11/787.0	2.4050(13)	Chem. Commun., 2021,57,6907–6910.
		2.3973(13)	
		2.3336(8)	
		2.3336(8)	
[EP]MnCl <sub>4</sub>	7.98/1400.0	2.3987(8)	Chem. Commun., 2021,57,6907–6910.
		2.3709(8)	
		2.3497(8)	
		2.3243(8)	
[TMGD] <sub>2</sub> MnCl <sub>4</sub>	71.6/3767.6	2.373(2)	J. Mater. Chem. C, 2021, 9, 9952–9961.
		2.370(2)	
		2.360(2)	
		2.351(2)	
[EMMIM] <sub>2</sub> MnCl <sub>4</sub>	60.6/3880.0	2.3651(13)	J. Mater. Chem. C, 2021, 9, 9952–9961.
		2.3580(13)	
		2.3562(13)	
		2.3530(14)	
[TPA] <sub>2</sub> MnCl <sub>4</sub>	34/3450.0	2.3881(6)	J. Mater. Chem. C, 2021, 9, 9952–9961.
		2.3783(7)	
		2.3682(6)	
		2.3603(6)	
[Me <sub>3</sub> NVinyl] <sub>2</sub> [MnCl <sub>4</sub> ]	2/–	2.311(10)	RSC Adv., 2021, 11, 2329–2336.
		2.306(10)	
		2.303(10)	
		2.303(10)	
(C <sub>4</sub> NOH <sub>10</sub> ) <sub>2</sub> MnCl <sub>4</sub>	39/3360.0	2.4096(4)	Chem. Sci., 2019, 10, 3836–3839.
		2.3703(4)	
		2.3600(4)	
		2.3450(4)	
(C <sub>7</sub> H <sub>13</sub> N <sub>2</sub> ) <sub>2</sub> MnCl <sub>4</sub>	70.78/3900	2.3613(9)	Dalton Trans., 2019, 48, 17451–17455.
		2.3556(9)	
		2.3511(9)	
		2.3503(10)	
(N-methyl-piperidinium)MnCl <sub>4</sub>	79.37/714.5	2.3945(11)	Inorg. Chem. Front., 2018, 5, 2615–2619.
		2.3570(11)	
		2.3567(11)	
		2.3374(10)	
(N-methyl-pyrrolidinium)MnCl <sub>4</sub>	1.27/156.2	2.3918(14)	Inorg. Chem. Front., 2018, 5, 2615–2619.
		2.3599(14)	
		2.3488(16)	
		2.3408(16)	
[(btz) <sub>2</sub> (MnCl <sub>4</sub> )]·2H <sub>2</sub> O	43.17/–	2.3828(13)	J. Fluoresc., 2016, 26, 2295–2301.

		2.3704(13)	
		2.3658(13)	
		2.3565(12)	
Mn <sub>3</sub> Cl <sub>6</sub> (18-crown-6) <sub>2</sub>	20/–	2.4282(14)	J. Am. Chem. Soc. 2021, 143, 798–804.
		2.3735(16)	
		2.3571(16)	
		2.3461(16)	
MnCl <sub>2</sub> (15-crown-5)	39/–	···	Inorg. Chem. 2021, 60, 14645–14654.
(KC) <sub>2</sub> MnCl <sub>4</sub>	7.79/2790.0	2.3983(12)	J. Am. Chem. Soc., 2019, 141, 15755–15760.
		2.3861(14)	
		2.3585(13)	
		2.3432(13)	
		2.3954(11)	
		2.3935(13)	
		2.3571(13)	
		2.3496(13)	
Mn(15-Crown-5)	68/1.41	2.139(8)	<b>This work</b>
(MnCl <sub>4</sub> )(DMF)		2.538(3)	
		2.421(3)	
		2.339(3)	
		2.343(3)	
		2.314(4)	